

Catalytic membrane reactors for methane reforming using hydrogen permselective silica membranes

T. Tsuru, K. Yamaguchi, T. Yoshioka and M. Asaeda

Hiroshima University, Department of Chemical Engineering, Japan
Higashi-Hiroshima 739-8527, JAPAN

Phone: +81-824-24-7714; Fax: +81-824-24-5494

E-mail: tsuru@hiroshima-u.ac.jp

Catalytic membrane reactors, consisting of a silica microporous layer and a Ni-catalyst layer, were prepared for the application of steam reforming of methane. Ni-catalysts were impregnated inside α -alumina supports (average pore size: 1 μm ; outer/ inner diameter: 10/ 8 mm; length 9 cm), followed by coating microporous silica layers for hydrogen separation on the outer surface of the Ni-impregnated supports. Catalytic membrane reactors showing hydrogen selectivity over nitrogen of 30-100 with hydrogen permeance of $1\text{-}10 \times 10^{-6} \text{ m}^3(\text{STP})\text{m}^{-2}\text{s}^{-1}\text{kPa}^{-1}$ were applied to the steam reforming of methane with addition of a small amount of oxygen. The reaction was carried out at 500 $^{\circ}\text{C}$, and feed and permeate pressure were kept at 100 kPa and 20 kPa, respectively. The ratio of feed flow rate of steam to CH_4 (S/C) was kept at 3, while that of oxygen to CH_4 (O/C) was controlled at 0 or 0.2. Methane conversion was increased upto 0.8 beyond the equilibrium (0.44 on the present condition) with hydrogen extraction. Steam reforming of methane with hydrogen extraction showed a lower temperature along the catalytic membranes, especially in inlet region of the catalytic membrane, than without hydrogen extraction, suggesting that steam reforming reaction of endothermic reaction was enhanced by hydrogen extraction. The experimental results (conversion and hydrogen recovery) showed a reasonably good agreement with the simulations of a co-current, isothermal and plug-flow-type membrane reactor.

Key words: catalytic membrane reactor, methane steam reforming, porous silica membranes, hydrogen

1. INTRODUCTION

Production of hydrogen by reforming of methane is limited, since the main reaction of methane reforming, that is, the steam reforming of methane (SRM) $\text{CH}_4 + \text{H}_2\text{O} = \text{CO} + 3\text{H}_2$, and the water shift reaction $\text{CO} + \text{H}_2\text{O} = \text{CO}_2 + \text{H}_2$ are subject to the thermodynamic equilibrium. A number of studies of membrane reactors for methane steam reforming using dense membranes such as palladium have been reported [1], while a limited number of papers have reported on membrane reactors for methane reforming that use porous membranes: steam reforming of methane using alumina membranes [2] and silica membranes [3, 4], and CO_2 reforming of methane using microporous silica membranes [5]. Membrane characteristics such as the permeabilities of hydrogen, water vapor, and methane, crucial factors that influence the performance of membrane reactors, have not been extensively investigated. Additional experimental investigations of membrane reactors using porous membranes would be important from the viewpoint of the dependency of the performance of membrane reactors on operating conditions (flow rate, pressure).

Another important factor is that SRM reaction is endothermic. The possibility of an autothermal reaction,

that is, a self-sustaining reaction in terms of reaction heat, was pointed out for the case of the SRM reaction with added oxygen (OSR) in a palladium membrane reactor [6].

In this study, catalytic membrane reactors, consisting of a silica hydrogen separation layer on Ni-catalyst impregnated substrates, were prepared and used for methane steam reforming with the addition of oxygen.

2. EXPERIMENTAL

The nickel catalyst was impregnated by immersing an α -alumina porous substrate (pore size 1 μm , outer diameter 10 mm, inner diameter 8 mm, length 9 cm) in the nickel nitrate solution, followed by firing at 500 $^{\circ}\text{C}$ in air. The hydrogen separation layer was then formed on the outer surface of the substrates [3, 4]. Catalytic membranes were fired in air at 500 $^{\circ}\text{C}$, and reduced to the elemental state by treatment with hydrogen at 500 $^{\circ}\text{C}$ prior to use [3].

A mixture of methane and steam ($\text{H}_2\text{O}/\text{CH}_4 = 3$) was continuously supplied to the catalytic membranes at a methane flow rate of approximately $0.5\text{-}20 \times 10^{-6} \text{ mol s}^{-1}$. The feed stream was approximately atmospheric, while the permeate stream was evacuated down to

approximately 20 kPa using a diaphragm pump. The reaction was carried out at 500 °C. Reactant gaseous mixtures were fed to the inner stream of the cylindrical membranes. Gas compositions were determined using two types of on-line gas chromatographs: GC-1 and GC-2. GC-1, equipped with a packed column of Gaschrompack 54 at an operating temperature of 180 °C was used for the analysis of water vapor and CO₂, while GC-2 with Molecular-Sieves operated at 80 °C was used for other gases such as H₂, N₂, and CO. The material balance of carbon, hydrogen, and oxygen atoms was within the maximum errors less than 10 %.

3. RESULTS AND DISCUSSION

3.1 Catalytic membranes

Figure 1 shows a cross-section of a catalytic membrane. An intermediate layer can be observed on the outer surface of the substrate with a thickness of approximately 1~2 μm. The top layer, which functions for hydrogen perm-selectivity, appears to be less than 1 μm. Nickel catalysts were observed on the α-alumina support. The average amount of Ni impregnation was approximately 0.25 g.

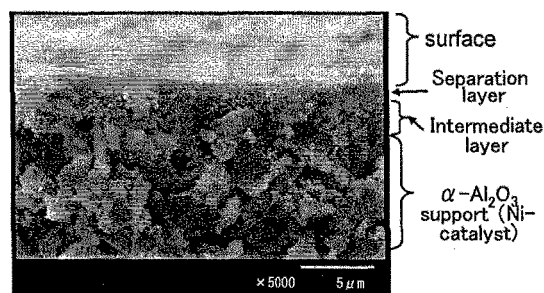


Fig. 1 Cross-section of a catalytic membrane

3.2 Effect of added oxygen on temperature profile of catalytic membranes

Figure 2 shows a temperature profile along the axis; the temperature of the outside of the membrane housing was maintained at 500 °C and the temperature inside the cylindrical membrane was measured by moving the location of the thermocouple inside the membrane. The temperature along the membrane axis was 500 ± 5 °C under conditions of N₂ flow. For the case of the SRM reaction without membrane permeation (SRM/ wP), the inside temperature, which was 490 °C at the inlet due to the endothermic reaction, increased along the axial direction and approached the same temperature profile as that for nitrogen flow, indicating that SRM occurred mainly in the first half of the membrane and no reaction occurred in the last half. With membrane permeation, the temperature decreased several °C. This indicates that the endothermic SRM reaction was enhanced by membrane permeation. For the case of OSR, the temperature was approximately 510 °C at the inlet, decreased drastically and then had approximately the same profile as that for N₂ flow especially in the last half of the catalytic membrane. No oxygen was detected in the permeate or retentate stream, suggesting that it was suggested that the exothermic reaction of methane

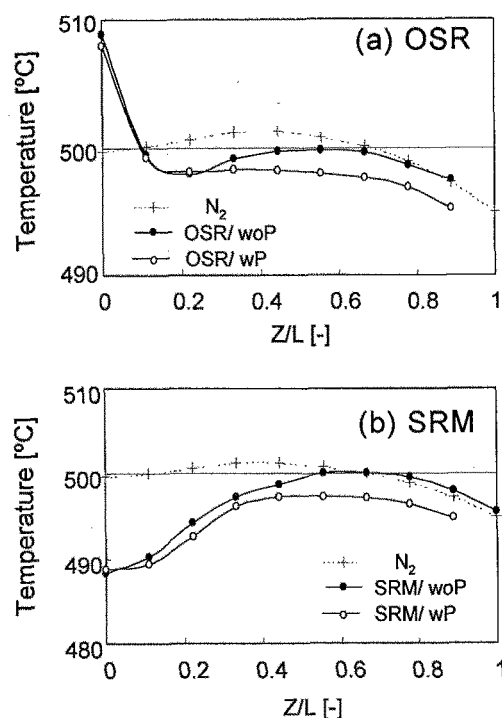


Fig. 2 Temperature profile along the axial direction for OSR (a) and SRM (b) (M-8; $F_{\text{CH}_4}=1.3 \times 10^{-5} \text{ mol s}^{-1}$; $S/C=3$, $O/C=0.2$; $p_{\text{H}}=100 \text{ kPa}$, $p_{\text{I}}=20 \text{ kPa}$)

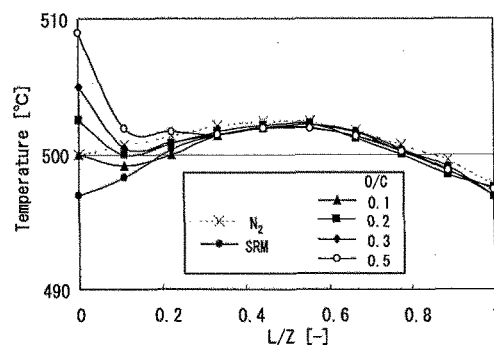


Fig. 3 Temperature profile along the axial direction for SRM and OSR without membrane permeation (M-8; $F_{\text{CH}_4}=3.8 \times 10^{-6} \text{ mol s}^{-1}$; $S/C=3$, $p_{\text{H}}=100 \text{ kPa}$)

combustion occurred near the inlet, followed by an endothermic steam reforming reaction. With membrane permeation, the temperature profile decreased by several °C, similarly to SRM.

Figure 3 also shows temperature profiles along the axis for the case of SRM and OSR without membrane permeation. The effect of the flow rate of oxygen on temperature profile under a constant CH₄ flow rate is shown in the figure. The inlet temperature of SRM reaction was approximately 497 °C, which is higher than the case of Fig. 2 due to a lower flow rate of methane. With an increase in O/C, in the range of 0 to 0.5, the temperature at the inlet increased from 497 to 508 °C. Therefore, temperature was found to be dependent upon both feed flow rate of methane and oxygen. Based on the temperature profile, it would be expected that the

reaction of methane reforming could be autothermal, if the controlled addition of oxygen along the catalytic membrane is possible.

Figure 4 shows the time course for the conversion and flow rate during steam reforming (SRM) and oxidative steam reforming (OSR) reactions with/ without membrane permeation. For the case of SRM, the conversion of methane without membrane permeation, which was achieved by closing the permeate stream, showed approximately the same value as the equilibrium conversion of 0.44 at 100 kPa, and increased with membrane permeation where the permeate stream was evacuated to approximately 20 kPa. It should be noted that the total flow rate was also increased with membrane permeation. For the case of OSR with an oxygen addition of $O/C=0.2$, the value for methane

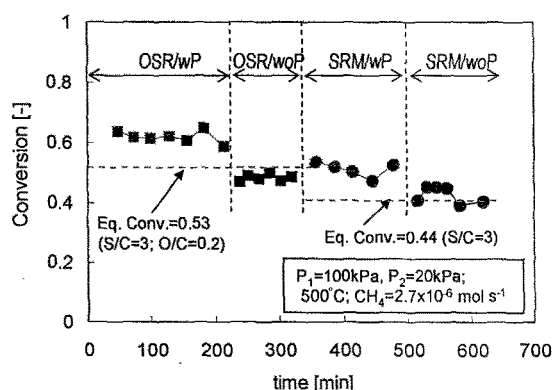


Fig. 4 Time course of CH_4 conversion for OSR and SRM with/ without H_2 permeation. ($P_1=100kPa$, $P_2=20kPa$; $S/C=3$; $500^\circ C$)

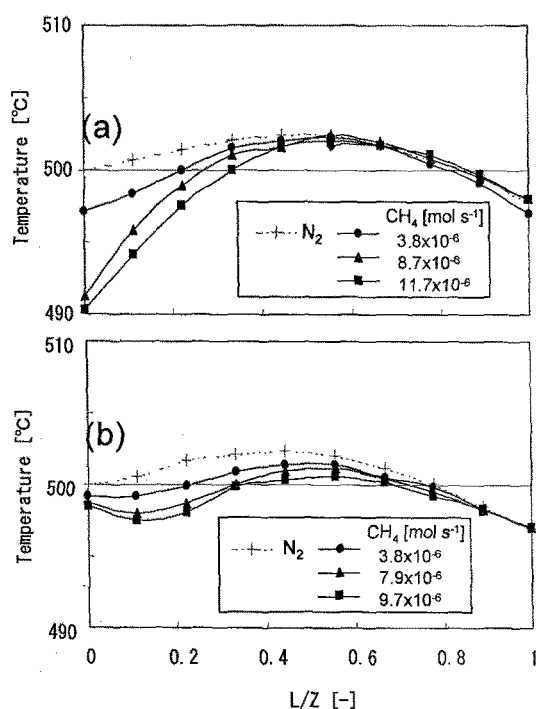


Fig. 5 Temperature profile along the axial direction for SRM without membrane permeation (fresh (a) and after 180h reaction (b))

conversion without membrane permeation was larger than that of SRM because of methane combustion, and increased with membrane permeation. In terms of total flow rate and permeate flow rate, the flow rates increased by membrane permeation.

3.3 Stability of catalytic activity

Figure 5 shows temperature profiles of a catalytic membrane fresh and after 180 hr reaction. Temperature decrease observed in the first half was obvious for the case of a fresh catalytic membrane, while that was not clearly observed after 180 hr reaction. This is probably caused by degradation of catalysts such as coking and sintering. Figure 6 shows SEM photos of impregnated catalyst of fresh, 180 hr, and long-term reaction. It is clear that Ni-catalysts of a fresh membrane was approximately $0.1 \mu m$ in size, and after long term reaction, the size was increased to $0.2-0.3 \mu m$, indicating degradation of catalytic activity was caused by sintering.

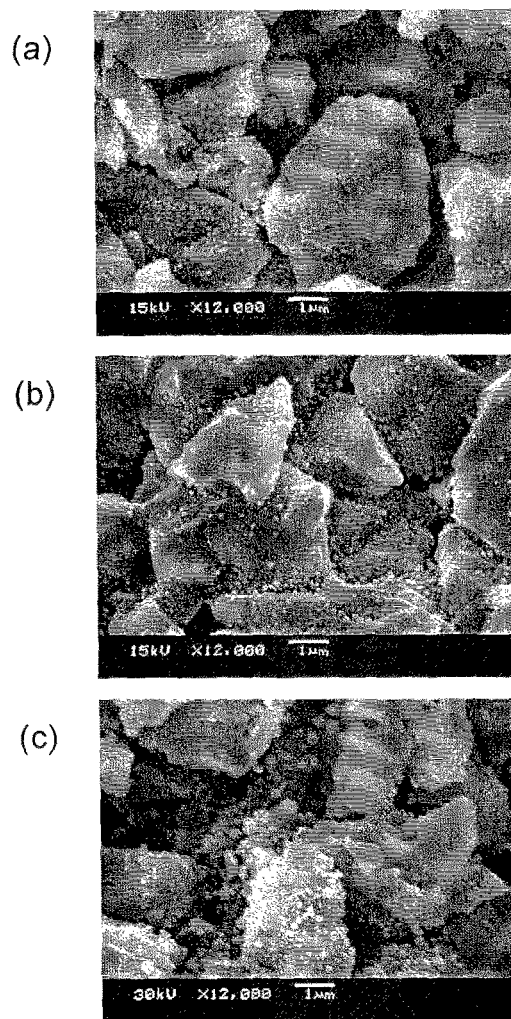


Fig. 6 SEM photos of catalyst. (fresh (a), after 180h reaction (b), and long term reaction (c).)

3.4 Catalytic membrane reaction

Figure 7 shows data on the conversion of methane, X_{CH_4} , hydrogen yield, Y_{H_2} , and flow rate of the retentate and permeate streams, when a microporous silica membrane, M-11, was used. Conversion without membrane permeation showed approximately an equilibrium conversion (0.44 on the present condition), indicating that the reaction rate was sufficiently high in the experimental ranges of methane feed flow rate. X_{CH_4} , which was increased with membrane permeation, and hydrogen yield, Y_{H_2} , increased to approximately 0.8 and 3, respectively, with a decrease in CH_4 feed flow rate.

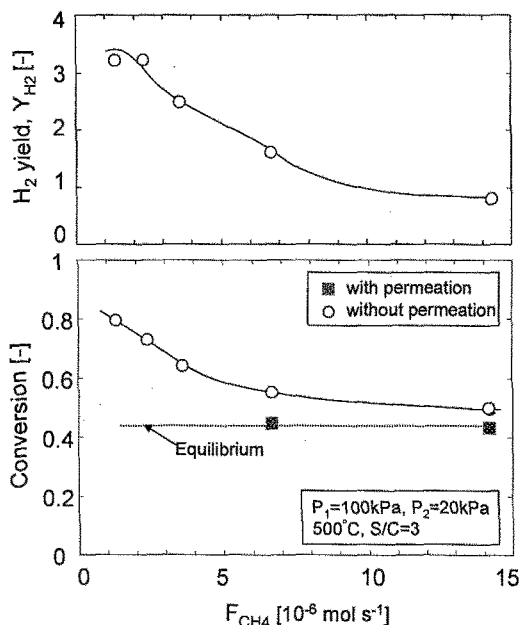


Fig. 7 Hydrogen yield, and CH_4 conversion as a function of CH_4 inlet flow rate (M11; SRM; $p_i=100$ kPa, $p_r=20$ kPa; $S/C=3$; $P(H_2)=5.9 \times 10^{-6} / 4.5 \times 10^{-6}$ $m^3 m^{-2} s^{-1} kPa^{-1}$, $\alpha(H_2/N_2)=87/69$ before/ after reaction; $\alpha(H_2/H_2O)=8$)

4. CONCLUSIONS

Methane steam reforming with and without oxygen addition was theoretically and experimentally investigated using microporous silica membranes, which allow the permeation of hydrogen as well as the feed and reactant gases based on permselectivity. Catalytic membrane reactors, consisting of a silica microporous layer and a Ni-catalyst layer, were prepared. Catalytic membrane reactors showing hydrogen selectivity over nitrogen of 30-100 with a hydrogen permeance of $1-10 \times 10^{-6}$ $m^3(STP)m^{-2}s^{-1}kPa^{-1}$ were applied to the steam reforming of methane. The reaction was carried out at 500 °C, and the feed and permeate pressure were maintained at 100 kPa and 20 kPa, respectively. Methane conversion, X_{CH_4} , increased up to approximately 0.8 beyond the equilibrium conversion of 0.44 by extracting hydrogen in permeate stream, and the permeated hydrogen yield, Y_{H_2} , reached a

maximum of 3 with membrane permeation.

5. ACKNOWLEDGEMENTS

This work was supported by a Grant-in-Aid for Scientific Research (B) from Japan Society for the Promotion of Science (JSPS) and the R&D Project for High Efficiency Hydrogen Production/Separation System using Ceramic Membranes funded by NEDO, Japan.

6. REFERENCES

- [1] Uemiya, S., N. Sato, H. Ando, T. Matsuda, and E. Kikuchi, *Appl. Catal.*, **67**, 223 (1991).
- [2] Tsotsis, T. T., A. M. Champagnie, S. P. Vasileiadis, Z. D. Ziaka, and R. G. Minet, *Sep. Sci. Tech.*, **28**, 397 (1993).
- [3] Tsuru, T., T. Tsuge, S. Kubota, K. Yoshida, T. Yoshioka, and M. Asaeda, *Sep. Sci. Tech.*, **36**, 3721 (2001).
- [4] Yoshida, K., Y. Hirano, H. Fujii, T. Tsuru, and M. Asaeda, *Kagaku Kougaku Ronbunshu*, **27**, 106 (2001).
- [5] Prabhu, A. K., and T. Oyama, *J. Membr. Sci.*, **176**, 233 (2000).
- [6] Grace, J. R., X. Li, and C. J. Lim, *Catal. Today*, **64**, 141 (2001).

(Received October 13 2003; Accepted March 31, 2004)